NATIONAL AERONAUTICS AND SPACE ADMINISTRATION

Technical Report 32-1251

Effects of Solar Proton Flares on the Power Output of Solar Cells Having Various Configurations

Paul Berman

JET PROPULSION LABORATORY
CALIFORNIA INSTITUTE OF TECHNOLOGY
PASADENA, CALIFORNIA

February 15, 1968

NATIONAL AERONAUTICS AND SPACE ADMINISTRATION

Technical Report 32-1251

Effects of Solar Proton Flares on the Power Output of Solar Cells Having Various Configurations

Paul Berman

Approved by:

L. D. Runkle for

P. Goldsmith, Manager
Spacecraft Power Section

JET PROPULSION LABORATORY
CALIFORNIA INSTITUTE OF TECHNOLOGY
PASADENA, CALIFORNIA

February 15, 1968

TECHNICAL REPORT 32-1251

Prepared Under Contract No. NAS 7-100
National Aeronautics & Space Administration

PRECEDING PAGE BLANK NOT FILMED.

Acknowledgment

The author is grateful to Dr. Bruce Anspaugh for performing the irradiations discussed in this report.

Page intentionally left blank

Page intentionally left blank

PRECEDING PAGE BLANK NOT FILMED.

Contents

Tables

Figures

Abstract

In designing a photovoltaic power system for deep space missions it is necessary to allow for degradation of the electrical output caused by exposure to solar proton flares. A technique for predicting the degradation of solar-cell power output for P/N and N/P silicon solar cells for two solar flare models is presented. The results of an experiment conducted to test the validity of the technique are also presented. The proton energies of 36, 100, and 137 MeV were used in the experiment. For protons of these energy levels, at a fluence of 2×10^{10} protons/cm^2, the only measurable electrical degradation occurred in the solar cell and not in the coverglass or coverglass adhesive. In general, the predictions were in reasonable agreement with the experimentally observed electrical degradations, but were pessimistic by approximately 6 to 9 and 3 to 6% for P/N and N/P cells, respectively. Some possible explanations for these discrepancies are given.

Effects of Solar Proton Flares on the Power Output of Solar Cells Having Various Configurations

I. Introduction

An appreciable amount of solar cell power degradation can occur as a result of exposure to solar proton fluxes. If not taken into account, this power degradation can result in failure of the power system to perform its function. It is the purpose of this report to discuss the effects of solar proton flares on N/P and P/N cells fabricated from 1-Ω-cm base material and with coverglasses of various thicknesses applied to the active face of the cell. The solar protons are considered to be omnidirectional within a plasma that moves through space. The most useful results of this investigation are figures which show the degradation of solar cell maximum power as a function of solar proton flares for nominal 1-Ω-cm resistivity N/P and P/N cells with 6-, 20-, and 60-mil thick coverglasses for two different models of the solar flare energy spectrum. The power degradation is presented as a function of the number of protons per square centimeter having an energy greater than 30 MeV. This is a convenient functional relationship because such data are available in much of the literature on solar proton flares.

The curves are obtained by relating the damage inflicted by protons as a function of proton energy to the fluence of 1-MeV electrons required to produce the same amount of damage for the various cell configurations considered, as first suggested by Rosenzweig (Ref. 1). Therefore, for any proton fluence energy spectrum, the equivalent number of 1-MeV electrons can be obtained. This, in turn, is used in conjunction with empirically determined curves, which relate the fluence of 1-MeV electrons to the resultant degradation of maximum power, to determine the power degradation that would occur after exposure to the proton flare considered.

Silicon solar cells of various configurations were irradiated at the Harvard University Synchrocyclotron with protons having energies of 36, 100, and 137 MeV to study the effects on the cell electrical characteristics and to determine the accuracy of the prediction techniques. The fluence at each energy was of the order of 2×10^{10} protons per cm^2.

Pre- and post-irradiation electrical tests were made in a solar simulator manufactured by Optical Coating Laboratories, Inc. (OCLI) and in a tungsten simulator to determine the amount of permanent electrical degradation. Transient effects were monitored by means of a mercury vapor lamp or a 150-W tungsten bulb. The results indicate that N/P 1-Ω-cm cells are approximately 7 to 10% higher in P/P_0 (power after exposure to power before exposure) ratio than the P/N cells when exposed to protons of these fluxes and energies. Similarly, the data roughly indicate that it takes approximately three to five times the fluence of protons at these energies to obtain the same percentage power degradation for nominal 1-Ω-cm N/P cells as for P/N cells. This is somewhat smaller than the factor of 6 usually quoted in the literature; however, the spread of data could account for this small difference. The data indicate that the theoretical predictions of the P/P_0 ratio at these proton energies and fluences were conservative by approximately 6 to 9 and 3 to 6% for P/N and N/P cells, respectively.

A. Theoretical Considerations

Calculations of the degradation of P/N cells under solar flare conditions were made utilizing Rosenzweig's curves (Ref. 2) for the correlation between proton damage as a function of energy and the equivalent 1-MeV electron fluence necessary to achieve the same power degradation. It is possible to obtain such curves because, in general, most of the degradation in the solar cell electric parameters can be related to changes in the minority carrier diffusion length in the base region of the cell (Ref. 3). These changes in minority carrier diffusion length can, in turn, be related to a damage coefficient which is characteristic of the type of irradiating particle, the particle energy, and the physical properties of the silicon.

The physical properties of the silicon are quite important in determining the radiation characteristics of the cell since the effect of recombination centers formed by radiation-induced defects and the minority carrier diffusion length can be strongly influenced by trapping levels which occur because of already existing structural or chemical imperfections. Therefore, while the number of radiation-induced defects for a particular type of particle radiation is quite similar for various types of silicon cells, the resultant electrical degradation is a function of how these radiation-induced defects associate themselves with the existing imperfections to reduce the minority carrier diffusion length. It would, therefore, be expected that a difference in impurity doping (e.g., phosphorus doping as opposed to boron doping) could give rise to differences in the damage coefficient.

After the damage coefficient for an ionized particle of a particular type is known (usually experimentally determined), the change in minority carrier diffusion length with fluence can be determined from the relationship quoted in Ref. 1.

$$\frac{1}{L_1^2} = \frac{1}{L_0^2} + K_1 \Phi_1 \qquad (1)$$

where

L_1 = diffusion length after irradiation by fluence Φ_1

L_0 = initial diffusion length

K_1 = damage coefficient

Φ_1 = fluence of particles

Other types of degradation can occur as the result of exposure to nuclear particle radiation, such as surface damage or damage to the P/N junction region. However, for the proton energies and coverglass thicknesses under consideration, these effects are negligible, and were not considered in this analysis. Hence, the electrical degradation, which is assumed to be only a function of L^2, can be obtained. If K is known for another type of particle, the Φ needed to obtain equivalent electrical degradation can then be determined from Eq. (2).

$$\frac{1}{K_2}\left(\frac{1}{L_1^2} - \frac{1}{L_0^2}\right) = \Phi_2 \qquad (2)$$

where

K_2 and Φ_2 = values appropriate to the second type of particle

L_1 = the value appropriate to the first type of particle

To obtain his curves, Rosenzweig utilized experimental data obtained on N/P silicon cells fabricated from 1-Ω-cm resistivity material. Therefore, the curves are appropriate only to this cell type and cannot be used directly for P/N cells. To accurately generate curves appropriate to P/N cells, a significant amount of data on the effects of proton irradiation on P/N cell current-voltage characteristics as a function of proton energy should be obtained. At present, little data are available because most of the proton experiments have been concerned with the more radiation-resistant N/P configuration. Consequently, in this analysis, the existing P/N data were correlated to the more extensive N/P data to obtain a curve which relates the equivalent 1-MeV electron fluence to the energy of a proton for P/N cells. The method of correlation is shown below:

Substituting $\frac{1}{L_1^2} - \frac{1}{L_0^2} = K_1 \Phi_1$ from Eq. (1) into

Eq. (2) gives

$$\frac{K_1 \Phi_1}{K_2} = \Phi_2 \tag{3}$$

where

Φ_1 = proton fluence at energy E

K_1 = damage coefficient for protons of energy E

Φ_2 = 1-MeV electron equivalent fluence

K_2 = damage coefficient for 1-MeV electrons

Then the equivalent 1-MeV electron fluence for 1 proton of energy E for P/N and N/P cells is given by:

$$\Phi_2 \,(N/P) = \frac{K_1 \,(N/P)\, \Phi_1 \,(N/P)}{K_2 \,(N/P)} \tag{4}$$

$$\Phi_2 \,(P/N) = \frac{K_1 \,(P/N)\, \Phi_1 \,(P/N)}{K_2 \,(P/N)} \tag{5}$$

where

$$\Phi_1 \,(N/P) = \Phi_1 \,(P/N) = 1$$

respectively. Dividing Eq. (5) by Eq. (4) gives

$$\frac{\Phi_2 \,(P/N)}{\Phi_2 \,(N/P)} = \frac{K_1 \,(P/N)\, K_2 \,(N/P)}{K_2 \,(P/N)\, K_1 \,(N/P)} \tag{6}$$

or

$$\Phi_2 \,(P/N) = \frac{K_1 \,(P/N)\, K_2 \,(N/P)}{K_2 \,(P/N)\, K_1 \,(N/P)} \Phi_2 \,(N/P) \tag{7}$$

It has been found experimentally (Refs. 3 and 4) that

$K_2 \,(P/N) \approx 2.3 \times 10^{-9}$

$K_2 \,(N/P) \approx 1.7 \times 10^{-10}$

$K_1 \,(P/N) \approx 6.2\, K_1 \,(N/P)$ at each energy

Substituting these values into Eq. (7) gives

$$\Phi_2 \,(P/N) = \frac{6.2\, K_1 \,(N/P) \times 1.7 \times 10^{-10}}{K_1 \,(N/P) \times 2.3 \times 10^{-9}} \Phi_2 \,(N/P)$$

$$= 0.46\, \Phi_2 \,(N/P) \tag{8}$$

Therefore, the equivalent 1-MeV electron fluence for a proton of energy E incident upon a P/N cell is 0.46 times the equivalent 1-MeV electron fluence for the same proton incident upon an N/P cell. Figure 1, Curve 1,

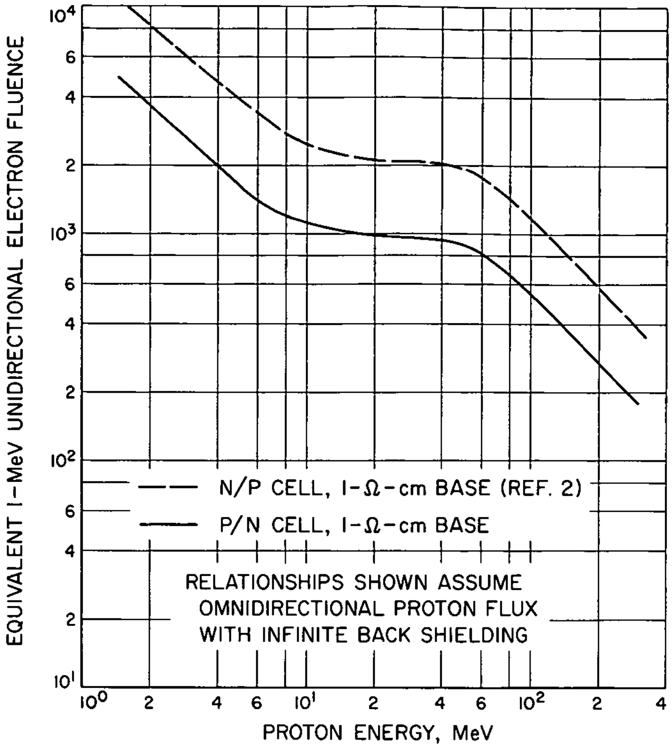

Fig. 1. Equivalent 1-MeV electron fluence as a function of proton energy

which shows the equivalent electron fluence per proton for N/P solar cells as a function of the proton energy, as obtained from Ref. 2, was used to determine the equivalent 1-MeV electron fluence for P/N cells as a function of proton energy and this relationship is shown as curve 2 of Fig. 1. As in Ref. 4, the correlation was made by assuming that the damage coefficient for N/P cells equals 6.2 times the damage coefficient for N/P cells at each proton energy level.

Two different models of the proton fluence as function of proton energy for a typical solar proton flare were considered. Model 1 assumes a linear relationship between the logarithm of the proton fluence having energy greater than a particular value E and the logarithm of the energy E and that there are seven times as many protons which have energies greater than 4.5 MeV (the energy cutoff point for 6-mil-thick quartz) as there are with energies above 30 MeV. Model 2 was developed by E. Divita of JPL[1]. This model, based on a compilation of experimental data from a number of references, does

[1]Private communication (July 12, 1966) on estimates of the proton fluences expected in the solar flare radiation environment during the *Mariner* 1969 mission to Mars.

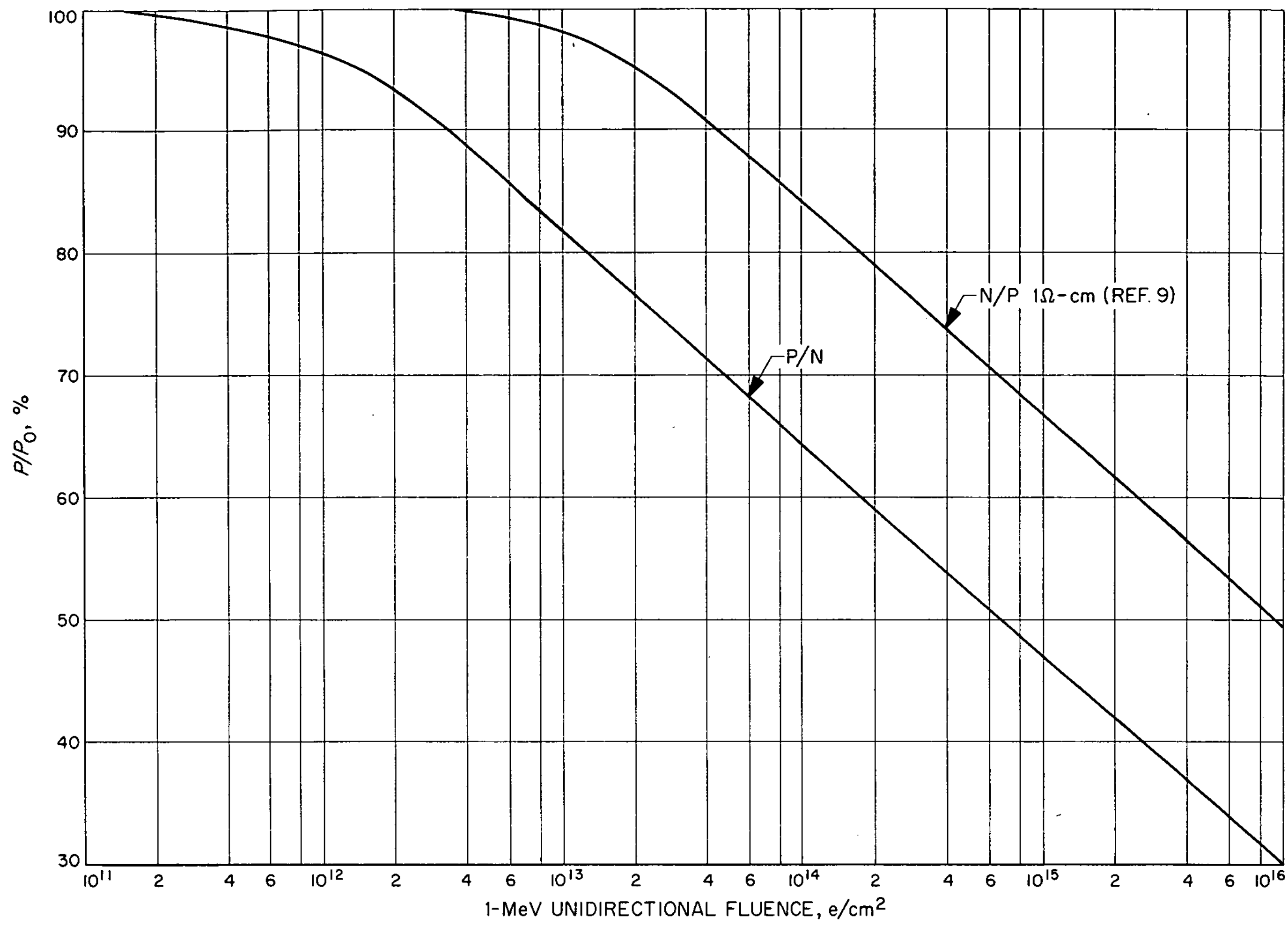

Fig. 2. Percentage of power remaining after exposure to 1-MeV electrons as a function of fluence for N/P and P/N 1-Ω-cm cells

not quite have the linear-logarithmic relationship assumed in Model 1, and indicates that there are 12 times as many protons with energies greater than 4.5 MeV as there are with energies greater than 30 MeV. Therefore, the second model gives a much larger total integrated proton fluence than the first model for a flare having a particular fluence of protons with energies greater than 30 MeV. Most of the extraterrestrial experimental data on solar proton flares do not consider particles with energies much less than 30 MeV so that it is convenient to relate degradation calculations to the number of protons with energy greater than 30 MeV.

Figure 1, which shows the equivalent 1-MeV electron fluence as a function of proton energy for P/N and N/P cells, was utilized in conjunction with the Model 1 and Model 2 proton flare spectra (assuming a proton energy cutoff appropriate to the thickness of coverglass being considered) to obtain an equivalent total 1-MeV electron fluence for each of the cell–coverglass combinations considered. This total 1-MeV electron fluence was converted into P/P_0 (power after exposure to initial power) ratio by means of the experimental relationships shown in Fig. 2. The P/P_0 ratio for the various cell–coverglass combinations for the Model 1 and Model 2 proton spectra are shown as a function of proton fluence above 30-MeV energy in Figs. 3 and 4, respectively.

Several limitations should be noted when using these figures. First, infinite back shielding of the solar cells was assumed. If this is not nearly the case, additional radiation will penetrate the cells through the substrate, resulting in additional degradation. In general, this is not expected to be a large effect, since the power degradation is, for the most part, linear with the logarithm of the fluence. Therefore, in the worst case, if there were no shielding on the backside (i.e., no substrate), the fluence incident upon the cells would be doubled. Figures 3 and 4 show that this would result in an additional degradation of approximately 5%.

The second limitation is that the curves are applicable only to high-efficiency cells (air mass zero efficiencies of approximately 10.5 and 11% for P/N and N/P cells, respectively, at a temperature of 28°C), i.e., to cells having relatively long initial diffusion lengths. Cells having short initial diffusion lengths will exhibit far less percentage degradation of power than shown in these figures. This is because $1/L_0^2$ of Eq. (1) is much greater than $K_1\Phi_1$ during initial exposure and, hence, $1/L^2$ is approximately equal to $1/L_0^2$ for relatively small values of Φ_1. Therefore, there will be little change in L until $K\Phi_1$ becomes significant with respect to $1/L_0^2$. If L_0 is small, $1/L_0^2$ will be large, and Φ will have to be higher to be of significance.

A comparison of Figs. 3 and 4 shows that the Model 2 flare results in a greater degree of power degradation than the Model 1 flare for an equivalent number of protons with $E > 30$ MeV. This is because the total integrated flux density of protons with $E > 4.5$ MeV is almost twice as large for the Model 2 spectrum. A significant difference in the effect of coverglass thickness also exists between the two models, especially with respect to the 20- to 60-mil coverglasses. For the Model 1 flare, the decrease in power degradation between 20- and 60-mil coverglasses is almost negligible, amounting to approximately 3%. Furthermore, even with a 60-mil coverglass, the P/N cell exhibits a larger power degradation than an N/P cell with only a 6-mil coverglass. For a Model 2 flare, however, a 60-mil coverglass gives a 6% decrease in the amount of power degradation over the degradation experienced with a 20-mil coverglass, and a P/N cell with a 60-mil coverglass shows less power degradation than an N/P cell with a 6-mil coverglass. These differences between the effect of the shield thickness for the two models can be easily understood and are consistent with theoretical expectations. The range of protons with energies above 17 MeV is greater than 60 mils in quartz so that it is highly probable that these protons will penetrate both 20- and 60-mil coverglasses. For a given total integrated proton flux, Model 1 indicates that approximately 25% of the protons will have energies in excess of 17 MeV, while Model 2 indicates that only approximately 15% of the protons will have energies in excess of 17 MeV. This says that for Model 1, 25% of the particles will be relatively unaffected by 60 mils of shielding, while for Model 2, only 15% of the particles will be unaffected. Figure 5 compares the effect of the two proton flare models from the point of view of degradation of maximum power as a function of coverglass thickness for N/P and P/N solar cells for solar proton flares having a total proton flux density with $E > 30$ MeV of 5.4×10^9 protons cm^{-2}, which, according to E. Divita of JPL[2], corresponds to the most intense six-month period yet recorded. This is approximately a factor of 2 higher than indicated in Ref. 5.

B. Experimental Considerations

Experimental proton irradiations were carried out at the Harvard University Synchrocyclotron so as to compare the theoretical predictions with experimental results and also to obtain information on the transient effects of high-energy proton irradiation. Three different energy levels were used for this investigation, i.e., 36, 100, and 137 MeV, and the fluences used were of the order of 2×10^{10} protons/cm^2. These higher energies were used because less information is available for these energies than for lower proton energies. Silicon solar cells of various configurations, and *Mariner* Venus 67, 7-cell submodules were considered in this experiment to isolate the regions of significant radiation damage to the submodules and to provide comparisons between the radiation effects of various cell designs. A group of cells composed of the items listed in Table 1 were irradiated at each of the three energy levels investigated.

[2]Private communication (July 12, 1966) on estimates of the proton fluences expected in the solar flare radiation environment during the *Mariner* 1969 mission to Mars.

Table 1. Experimental group irradiated at each energy level

Item	Quantity	Description
1	2	P/N *Mariner 67*, 7-cell submodules. Cells fabricated from 0.2 to 1.2 ohm-cm material
2	5	P/N (*Mariner 67*) filtered cells (6-mil coverslip) identical to cells of Item 1
3	5	P/N cells similar to Item 2 but without filters (bare)
4	5	P/N cells similar to Item 3 but with RTV coverslip adhesive applied to active face
5	5	N/P cells, 1 to 3 ohm–cm base resistivity, 6-mil coverglass
6	5	Coverslips
7	2	Coverslip-adhesive-coverslip sandwiches

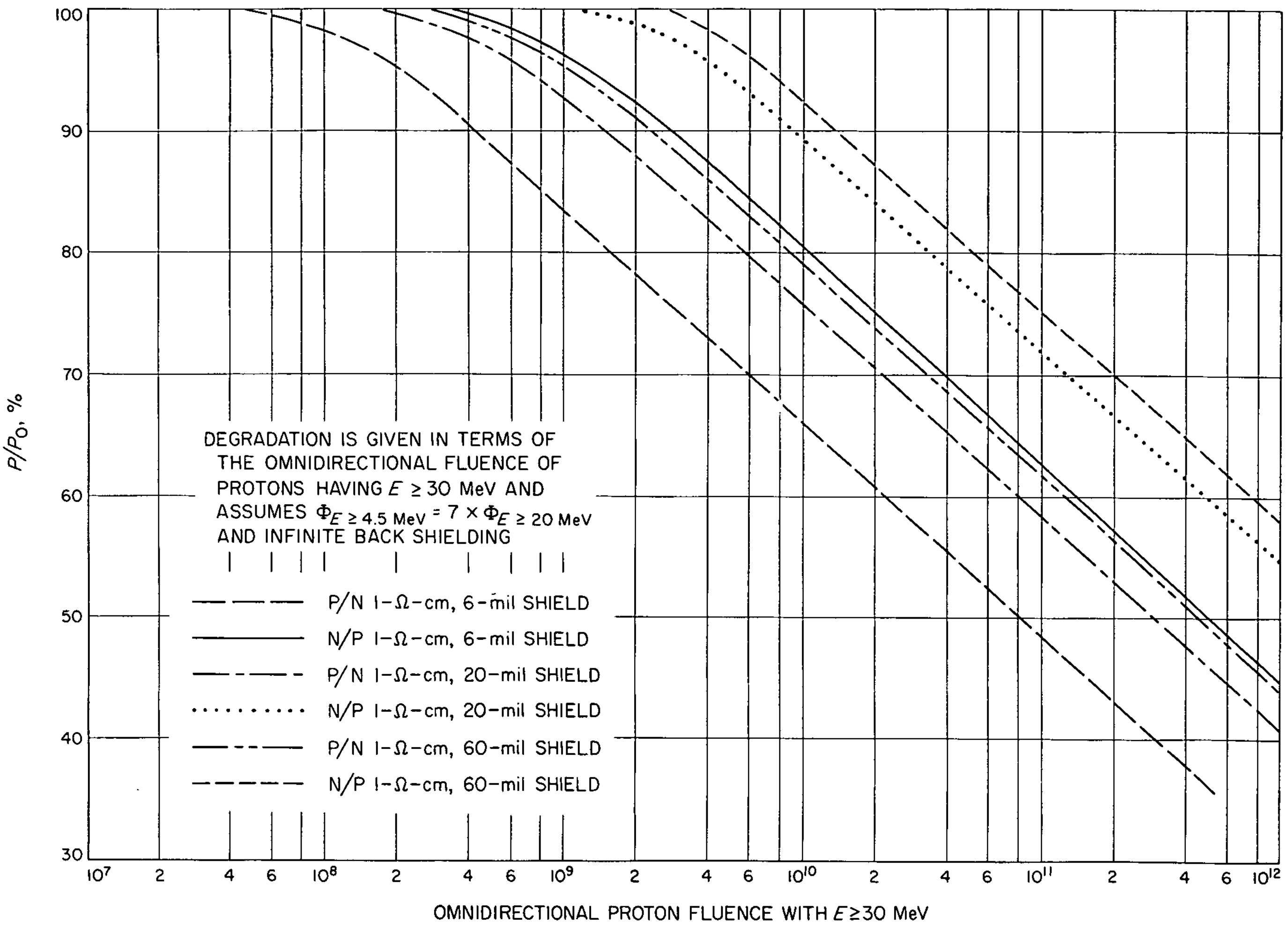

Fig. 3. Degradation of maximum power as a function of solar proton flares—Model 1

In Table 1, items 1 through 4, and 6 and 7 are directly applicable to the *Mariner* Venus 67 program. The N/P, 1 to 3-Ω-cm cells are applicable to *Mariner* Mars 1969. In addition to the above items, at each energy level, two P/N filtered cells and one N/P 8-mil-thick filtered cell were monitored under illumination during the proton irradiation to study transient effects. The test specimens were selected in such a way that any observed electrical degradation could then be traced back to effects in the coverslip, effects in the coverslip-adhesive combination, and effects in the cell itself.

The cells were mounted on an aluminum 1/16 × 15 × 15-in. plate. Three such plates, one at each energy level, were utilized. Provisions were made on the plates for illuminating the transient monitoring cells described above and for observing their short-circuit current output with a Simpson Meter Model 260 located in the control room.

As previously mentioned, three cells were monitored at each energy level under illumination. Since the short-circuit current portion of the characteristic current-voltage curve is the most sensitive to radiation damage, this parameter was observed during irradiation. Initially, it was felt that a light source having a high distribution of shorter wavelength (higher energy) photons should be used for illumination, since tungsten light, which emits a greater proportion of longer wavelength photons than sunlight, results in a greater sensitivity of the cell's electrical characteristics to radiation damage than would be the case in outerspace sunlight. This is because the long wavelength cell response is most drastically affected by ionized particle irradiation. During the experiment, however, no transient effects were observed, but a smooth permanent decrease in short-circuit current occurred. This was determined by periodically halting the irradiation and looking for a short-circuit recovery. Because of the lack of indicated transient effects, the mercury

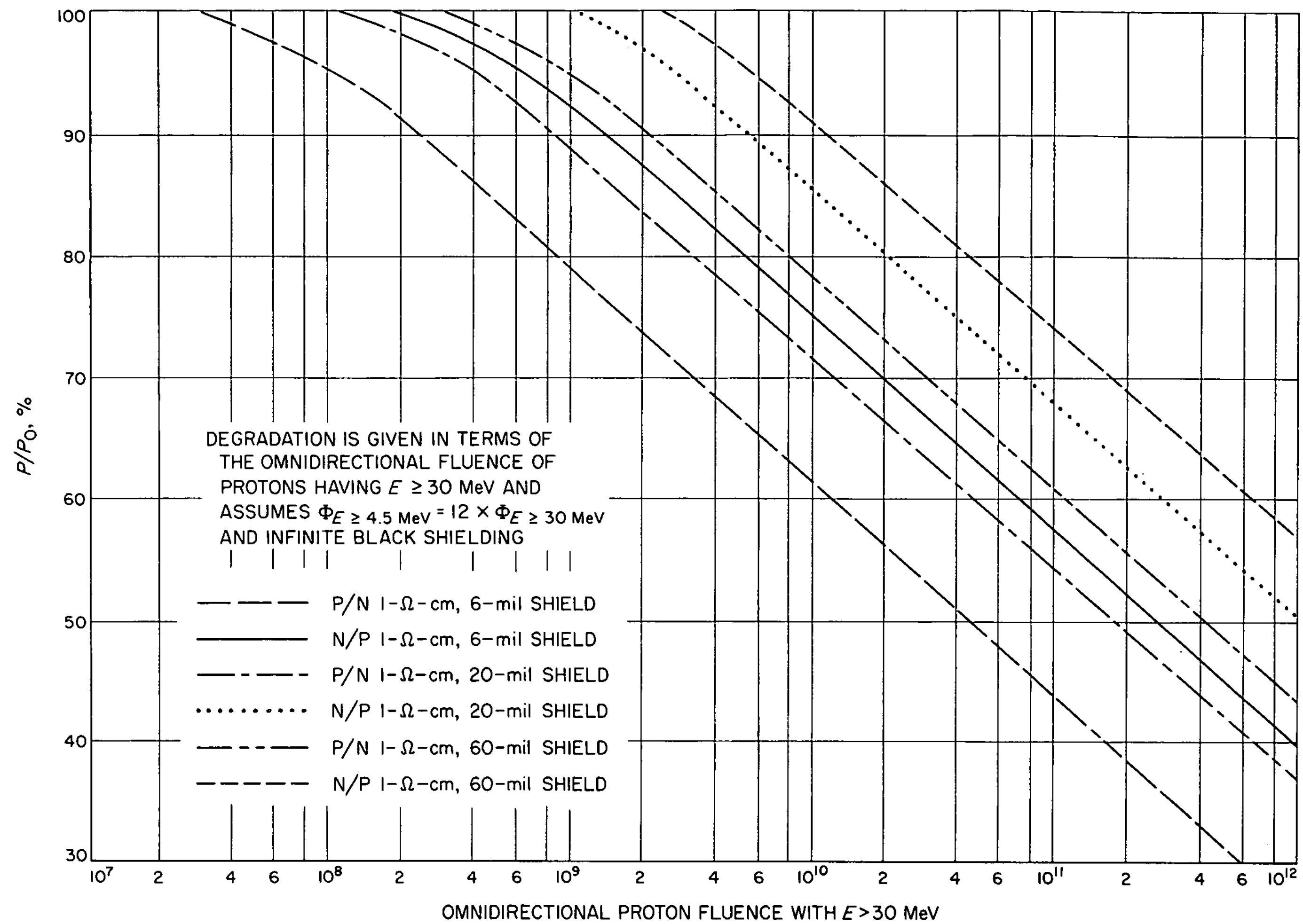

Fig. 4. Degradation of maximum power as a function of solar proton flares—Model 2

vapor lamp was replaced by a 150-W tungsten light source that magnified the degree of radiation degradation of the short-circuit current. The tungsten light source was used for the remainder of the 137-MeV irradiation and for the 100- and 36-MeV irradiations as well. Even with this light source, no transient effects were observed. Furthermore, the ratio of the short-circuit current to the initial short-circuit current showed the expected linear relationship to the logarithm of the fluence, which is characteristic of permanent degradation.

Pre- and post-irradiation current-voltage curves at a temperature of 28 ±2°C were obtained for each cell and for each submodule, as well as for two control submodules and several groups of control cells that were not irradiated, under illumination by an OCLI solar simulator calibrated to correspond to air mass zero solar spectrum, and under a tungsten simulator having a sunlight equivalent intensity of 100 mW/cm^2 and a color temperature of 2800°K. The OCLI simulator was set to correspond to an air mass zero solar spectrum by three balloon flight standard cells. One of the balloon flight standards had a 6000-Å band-pass filter bonded to the active face, while the other had an 8000-Å band-pass filter. The third standard had no band-pass filter, and was sensitive to light between 4500 and 1100 Å. The spectral distribution of the light was adjusted so that the ratio between the air mass zero balloon flight short-circuit current value and the short-circuit current value as measured in the simulator was identical for the three standard cells. Therefore, the relationship between the red portion of the spectrum, the blue portion of the spectrum, and the entire spectrum to which the solar cells are sensitive was the same as obtained during the balloon flights. It was found, by mapping the illuminated area, that it was necessary to reduce the intensity of the light to 80 mW/cm^2 to obtain a usable area over which the three balloon flight standards satisfied the desired

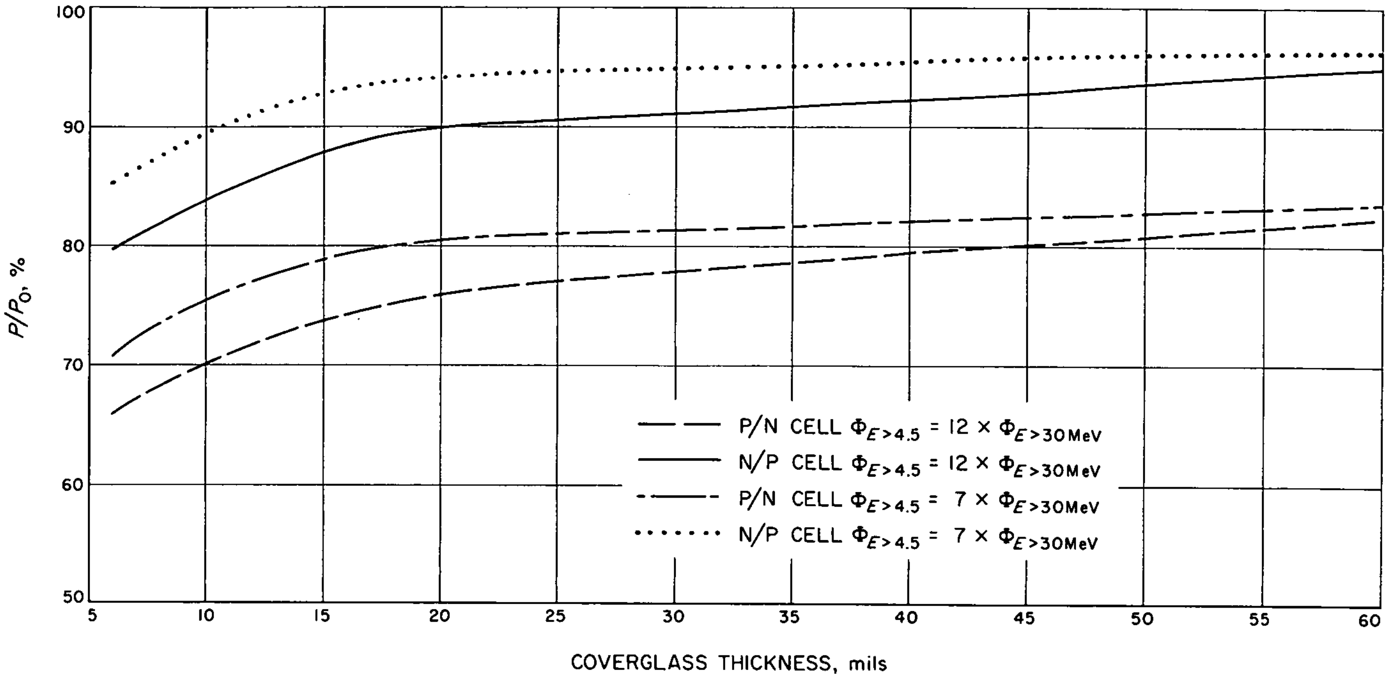

Fig. 5. Degradation of maximum power as a function of coverglass thickness for N/P and P/N cells for solar proton flare having 5.4 × 10⁹ P/cm² with E > 30 MeV (infinite back shielding)

condition. Therefore, although the spectral content of the simulator was similar to air mass zero, the intensity was reduced by a factor of approximately 0.57. This is not expected to significantly affect the results. A control solar cell was used as a detector cell for the coverslips and coverslip-adhesive sandwiches. Each of the filters and sandwiches was placed on top of the detector cell and the current-voltage curve of the cell was obtained.

C. Experimental Results

As previously mentioned, no transient effects were observed, even at flux rates as high as 10^7 protons-cm^2 (which are higher than the flux rates that would be expected because of solar flares). This observation was independent of whether a high-blue (mercury vapor lamp) or a high-red (tungsten lamp) illumination source was used.

The illumination from the OCLI solar simulator was uniform to ±2% over an area approximately 2 × 6 cm. The area of a 7-cell submodule is approximately 2 × 7 cm. When the post-irradiation measurements were made, the control (unirradiated) modules were approximately 4% lower in short-circuit current than the pre-irradiation values; therefore, these measurements are considered somewhat unreliable. A measurement accuracy (control cell reproducibility) of greater than 2% is desired for meaningful results. This was one of the reasons for utilizing the tungsten light source. Not only do the tungsten measurements provide a second set of independent measurements (the two illumination systems having been set up by different balloon flight standard cells), but the tungsten light source is extremely stable and has a large, uniform area of illumination. Unfortunately, the spectral content of the tungsten light is considerably different from natural sunlight, so that the results obtained under tungsten illumination must be used with discretion. It was expected, *a priori*, that the percentage of electrical degradation experienced by the P/N cells with the 6-mil coverglasses (item 2) would be identical to that experienced by the submodules (item 1). By comparing the pre- and post-radiation data obtained from the cells and submodules under tungsten light, which should magnify any differences, this expectation was found to be valid. A summary of the data is presented in Table 2.

It can be concluded that there is no significant difference in radiation damage between submodules and the individual cells from which the modules are made, for the proton energy levels considered in this experiment. The results obtained in the solar simulator for the P/N

Table 2. P/P_0 ratio for P/N cells and P/N submodules as measured in tungsten simulator

Sample	Proton energy level (MeV)	P/P_0 range
P/N with 6-mil coverslip (5 cells at each proton energy level)	36	0.73–0.80
	100	0.74–0.84
	137	0.82–0.88
	0	1.00–1.00
7-cell submodules (2 modules at each proton energy level)	36	0.76–0.78
	100	0.83–0.83
	137	0.84–0.85
	0	1.00–1.00

cells with 6-mil-thick coverslips are, therefore, applicable to submodules as well. The reproducibility of the control cell measurements in the simulator was quite good (the control cell readings were reproduced to better than 2%). Therefore, it may be concluded that the problem encountered in measuring the submodules in the simulator were simply caused by the large area of the module, which was somewhat beyond the capabilities of this particular simulator.

There was no significant damage done by the protons to the coverslips and the coverslip-adhesive sandwiches since the pre- and post-irradiation measurements were identical to within the ±2% measurement error.

A summary of the results obtained in the OCLI solar simulator is presented in Table 3. The table shows that the P/N cells with coverslips, without coverslips, and with adhesive only, exhibit similar electrical degradation as a result of the proton irradiation at any given energy level and, if desired, the results of the three types of P/N cells could be pooled to give a sample size of 15 units at each energy level. This bears out the results obtained from the coverslip and coverslip-adhesive sandwiches experiment; i.e., there is no significant damage, at least as far as the solar cell electrical characteristics are concerned, occurring in either the coverslip or the adhesive used to bond the coverslips to the active cell face. The electrical degradation is a result of damage to the cell for these energy ranges and fluences. Furthermore, the coverslip provides no significant attenuation of protons in these energy ranges, as is expected from the range-energy relationships.

Table 3. Electrical cell degradation (OCLI simulator) (5 cells of each type at each energy level)

Cell type	Proton energy, MeV	ISC/ISC_0 range	VOC/VOC_0 range	P/P_0 range
P/N (6-mil coverslip)	36	0.85–0.87	0.94–0.97	0.81–0.84
	100	0.86–0.91	0.96–0.97	0.83–0.88
	137	0.90–0.94	0.97	0.87–0.91
	0	1.00	0.98–1.00	0.98–1.00
P/N (no coverslip)	36	0.84–0.90	0.94–0.96	0.81–0.86
	100	0.89–0.92	0.95–0.97	0.85–0.90
	137	0.90–0.92	0.96–0.97	0.87–0.89
	0	1.00	0.99	0.98–0.99
P/N adhesive only	36	0.87–0.91	0.94–0.96	0.82–0.85
	100	0.87–0.92	0.96–0.97	0.85–0.88
	137	0.91–0.93	0.96–0.98	0.88–0.90
N/P 1-ohm-cm	36	0.95–0.96	0.97–0.99	0.92–0.94
	100	0.96–0.97	0.98–1.00	0.94–0.97
	137	0.97–0.99	0.98–0.99	0.95–0.98

D. Comparison Between Theoretical and Experimental Results

The equivalent 1-MeV electron fluxes as a function of proton energy shown in Fig. 1, are actually appropriate to an omnidirectional flux of protons with infinite back shielding of the cell; therefore, only one-half the total fluence is actually incident upon the cell. (This is normally the case for calculations involving solar protons, and thus the curves can be used directly.) In the case of this experiment, however, since there is a unidirectional flux of protons, the equivalent 1-MeV electron fluence determined from Fig. 1 must be multiplied by a factor of 2.

Figure 6 shows the results for the P/N and N/P cells with 6-mil-thick coverslips. The P/P_0 range for these two cell types is plotted as a function of the equivalent 1-MeV electron unidirectional fluence as determined from Fig. 1 with the factor of 2 correction. Also shown in this figure are the predicted degradation curves for the P/N and N/P cells. The experimental points for the P/N cells actually lie approximately midway between the predicted N/P and P/N curves and indicate that the lowest P/P_0 ratio observed was actually approximately 6% higher than the predicted P/P_0, i.e., the P/N cells were at least 6% higher in power than predicted. Similarly, the N/P cells were from 3 to 6% higher in power than predicted. Since the damage coefficients for the P/N cell were derived from those of the N/P cell using Rosenzweig's factor of 6.2 (Ref. 4) between the coefficients at each proton energy, it is not too surprising that the P/N prediction was off by a higher percent than the N/P prediction. A factor of 4, which is less conservative,

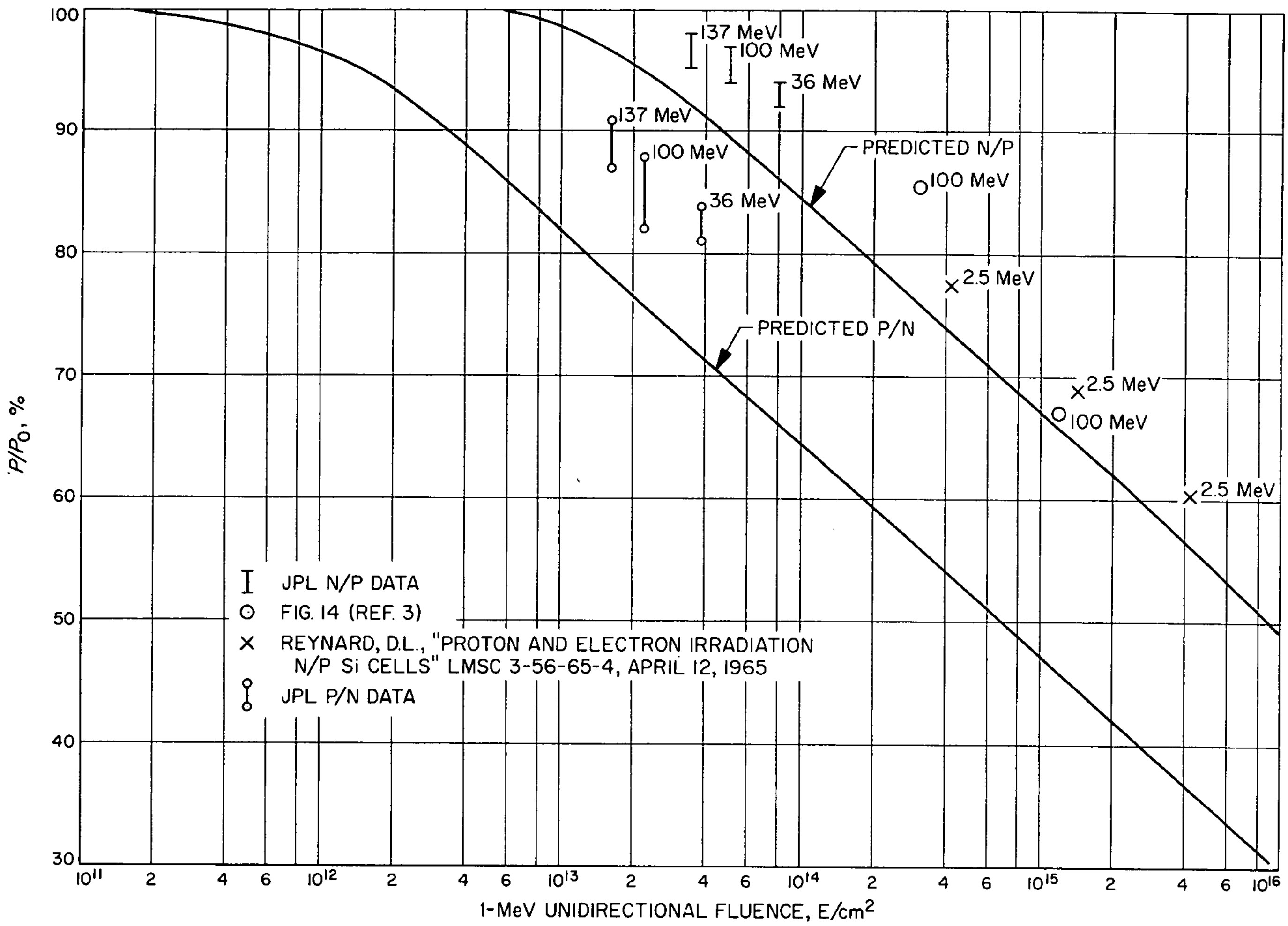

Fig. 6. Comparison between predicted and observed power degradation as a result of irradiation by protons having various energies and fluences

is quoted in Ref. 3. Utilization of this factor would bring the P/N predictions more in line with the N/P predictions. However, this still leaves a 3 to 6% discrepancy between the predicted and the actual P/P_0 ratio. While the prediction technique was geared to be somewhat on the conservative (pessimistic) side, it was felt that one reason for the discrepancy might have been an error in the dosimetry. If the dosimetry were such that the actual fluence was smaller than indicated, the points would be shifted toward the predicted curve. The data were compared with results presented in published data to ascertain whether the results of these experiments are reasonable. Most of the existing proton data were obtained on N/P cells (one of the reasons for conducting these investigations on P/N cells), and some of the published data for this cell type were plotted in Fig. 6. The P/P_0 ratio was obtained from the published data and the reported fluence was converted to equivalent 1-MeV electron fluence by utilizing Fig. 1. Most of the data points are greater than 3% in P/P_0 than the predicted curve. (The 100 MeV $- 5 \times 10^{11}$ P/cm^2 point is the only point which is closer to the predicted curve than 3%.) Then, the data of this experiment seem in reasonable agreement with past experimental data and it is unlikely that the discrepancy is caused by dosimetry.

Another possible reason for the pessimism of the predicted P/P_0 is that the damage coefficients determined by Rosenzweig (Ref. 2) may be pessimistic because they were obtained for low excess carrier densities, rather than at the much higher excess carrier densities appropriate to solar illumination. If it is assumed that the damage coefficients are too high by a factor of 2, and that

$$K_1\ (P/N) \approx 4\, K_1\ (N/P) \text{ at each energy}$$

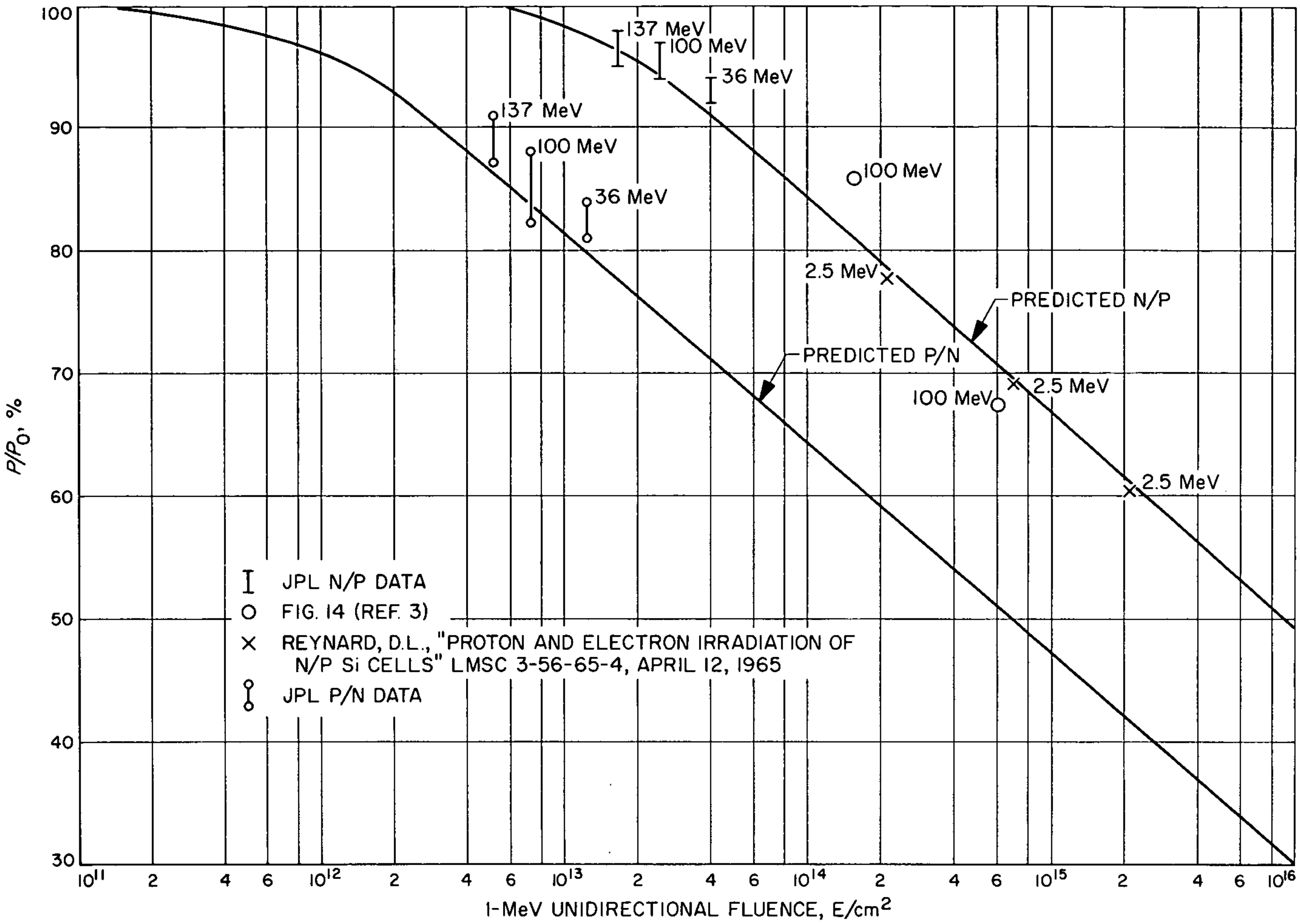

Fig. 7. Comparison between predicted and observed power degradation as a result of irradiation by protons having various energies and fluences using modified damage coefficients

as suggested in Ref. 3, the JPL experimental data, as well as other published data, are in very good agreement with the predicted values as shown in Fig. 7. This is encouraging because, on the basis of this limited study, it might be possible to obtain sets of damage coefficients which can quite accurately predict the power degradation of specific cell types.

II. Conclusions

The experiment indicated no significant transient effects over the range of proton energies considered, even with fluences as high as 10^7 protons/cm^2/s. It was also shown that the measurable electrical degradation is in the cell, rather than in the coverslip or in the coverslip adhesive, for protons of these energies and fluences. Also, for protons having these energies, there was no discernible difference in electrical degradation between cells with 6-mil-thick coverslips and cells without coverslips, as was expected from examination of proton energy-range relationships. It was shown that the electrical degradation of a solar cell module of the *Mariner* Venus 67 type can be accurately determined by obtaining the degradation of the cells from which the module is made.

Curves were generated, on the basis of presently available information, showing the amount of degradation that can be expected as a result of exposure to solar proton flares for various solar cell coverglass combinations. A number of simplifying assumptions were utilized. An experiment was carried out to provide information as to the validity of the technique used to generate the curves and, while in general the technique represented the experimentally obtained results, the predictions were actually pessimistic by approximately 6 to 9 and 3 to 6%

for P/N and N/P cells, respectively. Although a discrepancy of this magnitude is not unreasonable considering the problems of correlating experiments performed by one laboratory to those performed by another with respect to dosimetry, cell electrical measurements, and variations of radiation characteristics from cell batch to cell batch, additional possible explanations for these discrepancies were given. Furthermore, it was shown that, by manipulating the published data for radiation damage coefficients, the theoretical results can be brought into better agreement with the experimental results obtained by JPL, and also with the results of several other investigators. While this is quite encouraging, a considerable amount of additional work is necessary to generate enough data to show that these manipulations are justified. Further experiments of this nature would be helpful in making more accurate predictions of cell degradation caused by exposure to solar proton flares.

References

1. Rosenzweig, W., "Space Radiation Effects in Silicon Devices," *IEEE Trans. on Nuclear Science,* Oct. 1965.
2. Rosenzweig, W., "Results of the Tellstar Radiation Experiments," *Bell System Tech. J.*, Vol. 42, pp. 1548, 1963.
3. Cooley, W., Janda, R., and Shivanandan, K., *Handbook on Space Radiation Effects to Solar Cell Power Systems,* National Aeronautics and Space Administration, Contract NASw-598, July 22, 1963.
4. Rosenzweig, W., Smits, R. M., and Brown, W. L., "Energy Dependence of Proton Irradiation Damage in Silicon," *J. Appl. Phys.*, Vol. 35, No. 9, Sept. 1964.
5. Modisette, J., *et al., Model Solar Proton Environments for Manned Spacecraft Design,* NASA Report TD-2746, Manned Spacecraft Center, Houston, Texas, April 1965.
6. Cunningham, B. T., and Moss, E., *Post-Irradiation Room Temperature Electrical Characteristics of N/P Silicon Solar Cells,* National Aeronautics and Space Administration, Goddard Space Flight Center, Greenbelt, Maryland, Aug. 1964.